



Application of RCS and signal-free RCS to tree-ring width and maximum latewood density data

Inga K. Homfeld^{a,*}, Ulf Büntgen^{b,c,d}, Frederick Reinig^a, Max C.A. Torbenson^a, Jan Esper^{a,c}

^a Department of Geography, Johannes Gutenberg University, Mainz 55099, Germany

^b Department of Geography, University of Cambridge, Cambridge CB2 3EN, UK

^c Global Change Research Institute, Czech Academy of Sciences, Brno 613 00, Czech Republic

^d Department of Geography, Faculty of Science, Masaryk University, Brno 613 00, Czech Republic

ARTICLE INFO

Keywords:

Maximum latewood density
Temperature
Tree-ring width
Scandinavia

ABSTRACT

Dendroclimatic research faces the challenge of selecting appropriate detrending methods for retaining low-frequency signals in temperature reconstructions. Among the numerous methods available to dendrochronologists, regional curve standardisation (RCS) and the signal-free approach in combination with RCS (SF-RCS) are increasingly used to preserve the full spectrum of temperature variance in tree-ring data. Here, we apply RCS and SF-RCS to tree-ring width (TRW) and maximum latewood density (MXD) datasets composed of only living and combined living and relict trees from northern Scandinavia. Whereas RCS and SF-RCS produce highly similar chronologies when applied to composite (living-plus-relict) datasets, particularly for MXD, both methods fail to establish chronologies coherent with regional temperature trends when applied to living-tree datasets. Additional tests including pruning of well-replicated living-tree datasets, to approximate the heterogenous age-structure of composite datasets, reveal improved results and coherent trends in MXD. While this demonstrates the applicability of joint detrending and pruning techniques to retain meaningful low-frequency variance in living-tree MXD chronologies, similar improvements were not achieved with TRW, likely because of the much stronger age-trend inherent to this widely used proxy. Further tests with other tree species and in alpine environments are needed to verify these findings. However, such assessments require an adjustment of tree-ring sampling protocols to increase replication to 50+ trees per site including old and young individuals to facilitate data pruning.

1. Introduction

The removal of non-climatic information from tree-ring width (TRW) and maximum density (MXD) measurements is an important step in the development of climate reconstructions (Fritts, 1976). This process is commonly referred to as detrending, and numerous statistical approaches exist to estimate and remove the biological growth trends contained in TRW and MXD measurement series (Cook, 1987, 1985; Cook and Kairiukstis, 1990; Fritts, 1976). These tree-specific detrending methods can be grouped into two classes: one consists of deterministic methods fitting linear or curvilinear mathematical functions to the data (Fritts et al., 1969); and the other comprises stochastic or data-adaptive methods using low-pass filtering or smoothing splines (Cook and Peters, 1981). These detrending methods are, however, unable to ultimately distinguish non-climatic from climatic low-frequency variance in TRW

and MXD, leading to the potential removal of climatic information (Briffa et al., 1996; Melvin, 2004; Melvin and Briffa, 2008). This problem becomes especially evident when dealing with composite records combining living and relict samples, for which individual detrending methods may fail to retain long-term climatic trends on multi-centennial to millennial timescales (Esper et al., 2012a). Efforts to resolve this issue and reduce the loss of climatic information continue to produce new methods and best practice recommendations (Briffa and Melvin, 2011; Cook et al., 1995; Esper et al., 2003; Melvin and Briffa, 2008), adding to the multitude of detrending options and available software programs, each with specific requirements, benefits, as well as drawbacks.

Improved preservation of low-frequency signals is of key interest as it allows for the assessments of long-term climate evolution (Esper et al., 2016) and increases the accuracy of future climate change projections (Wilson et al., 2016). Several detrending issues, however, complicate the

* Corresponding author.

E-mail address: ihomfeld@uni-mainz.de (I.K. Homfeld).

accurate retention of low-frequency signals and require specific attention during data processing (Briffa et al., 1996; Briffa and Melvin, 2011; Cook et al., 1995). The so-called segment length curse describes the incapability of individual trees to reflect climate information beyond the length of the tree-ring sample, resulting in a loss of low-frequency information in mean chronologies (Cook et al., 1995). One widely applied method to tackle the segment length curse and preserve low-frequency information in TRW and MXD chronologies is regional curve standardisation (RCS; Briffa et al., 1992; Esper et al., 2003). Instead of individually fitting detrending curves to each measurement series, all series are aligned by cambial age, and a single growth curve is derived, which is smoothed using a statistical function. The resulting curve is then applied to detrend the measurement series before these are reassigned to their calendric date, and the chronology is produced (Esper et al., 2003). Most importantly, a larger number of both living and dead samples equally temporally distributed is required to accurately represent tree growth throughout time.

Most publicly available datasets from the International Tree Ring Database (ITRDB; Zhao et al., 2019) are shorter than 400 years (St. George, 2014), and the most common sampling design focused on mature and old trees at each site (Nehrbass-Ahles et al., 2014). This coherent age structure and parallel aging of a limited number of old trees limits the application of RCS, as the method's strength lies in comparing rings of the same cambial age that are distributed throughout a longer period of time (Esper et al., 2003). A more recently introduced detrending approach is the "signal free" (SF) approach (Melvin and Briffa, 2008), which incorporates established methods such as RCS. The application of SF-RCS has gained popularity as an alternative to classical RCS detrending applied to living-tree and composite datasets (Cooper et al., 2016; Matskovsky and Helama, 2014; Wang et al., 2014; Wilson et al., 2012; Zhang et al., 2015). SF-RCS involves an iterative process to estimate the detrending curve after removing the common climatic signal from the measurements (Melvin, 2004; Melvin and Briffa, 2008, 2014). One advantage of this combined approach compared to RCS is a reported decreased need for a wide temporal distribution of relict material (Melvin and Briffa, 2014). However, the improvements from applying SF-RCS to both TRW and MXD data as well as the limitations with living-tree datasets, compared to composite living and relict datasets, and methods to mitigate these have not been fully explored yet.

In this study, we assess RCS, SF-RCS, and classic individual-series detrending applied to temperature-sensitive TRW and MXD data from Northern Scandinavia and compare the resulting chronologies with long instrumental temperature series. Through adjusting sample age and replication of living-tree datasets, we mirror classical as well as composite sampling approaches, allowing a detailed investigation of RCS and SF-RCS detrending with respect to varying age structure and sample replication.

2. Material and methods

2.1. Tree-ring data and detrending

For a comparison of RCS-based detrending methods, the target dataset needed to fulfil several criteria: (i) high sample replication, (ii) strong temperature signal, and (iii) consist of a single species. While a high number of samples is required to investigate the effects of replication and age during detrending, a high-temperature sensitivity supports the translation of detrending effects on climate reconstructions and comparison with instrumental records. Finally, using a single species avoids bias possibly introduced through varying species-specific growth patterns and climate responses. A region that is ideally suited for such a comparison is Northern Scandinavia, hosting a long history of dendroclimatological studies with many temperature-sensitive records of various lengths (Büntgen et al., 2011; Esper et al., 2012a; Gunnarson et al., 2011; Linderholm et al., 2010; Melvin et al., 2013).

We selected two datasets, one consisting of living and sub-fossil *Pinus sylvestris* samples from the N-SCAN network (Esper et al., 2012a, 2012b) and a second collection of exclusively living trees from the same area and species (Fig. 1; Büntgen et al., 2011). The N-SCAN collection consists of 587 TRW and MXD series covering the period from 215 BCE to 2006 CE (Fig. 2) collected at 17 sites, three of which provide living-tree and 14 sub-fossil material. The exclusively living material originates from five sites including 792 TRW and MXD measurement series extending back to 1475 CE. Samples were processed following standard procedures and details can be found in the original publications (Büntgen et al., 2011; Esper et al., 2012a). All data were detrended using the ARSTAN version 41 and RCSsigFree version 45 programs (Cook, 1985; Cook et al., 2017a, 2017b). Average interseries correlation (r_{bar}) was calculated using Cofecha (Holmes, 1983), and all subsequent analyses were completed using RStudio (R Core Team, 2022), treeclim (Zang and Biondi, 2015) and dplR (Bunn, 2008).

The composite TRW and MXD data were RCS and SF-RCS detrended using residuals with power transformation, and ratios without power transformation (Cook and Peters, 1997). All detrendings considered the pith offset of each sample, had a 100-year smoothing spline applied to the regional curve, and used one of three variations of variance stabilization (none, RBAR based stabilization, RBAR and spline stabilization; Frank et al., 2007). The resulting 12 chronology versions for each method and parameter were averaged to create mean chronologies for each of the four groups: TRW RCS, TRW SF-RCS, MXD RCS, MXD SF-RCS (Supplementary Table S1).

The 792 samples of the five living-tree sites were merged (hereafter designated *full dataset*), as demonstrated in Büntgen et al. (2011), and a subset including only the oldest 69 samples with a minimum age of 250 years (hereafter *old dataset*) used to resemble the composition and age structure of classic dendroclimatological datasets. The full and old living-tree datasets were detrended using the same RCS and SF-RCS approaches as applied to the composite dataset to produce 12 chronology versions for each TRW and MXD. In addition, we applied negative exponential (NegEx) detrending using the same power transformation and variance stabilization variants, to add a classic method considered for datasets composed of only living trees. The different chronology versions (Supplementary Table S1) were again averaged to create mean curves: TRW/MXD NegEx, TRW/MXD RCS, and TRW/MXD SF-RCS.

In an attempt to emulate the age structure of a composite dataset, we used the full dataset truncated to rings older than 50 years and younger than 150 and produced a subset of only 527 (of the total of 792 living-tree) series including at least ten rings, hereafter referred to as the *pruned dataset*. This process mirrors the age-band decomposition procedure introduced by Briffa et al. (2001) to retain low-frequency variance in tree-ring chronologies (Römer et al., 2021), though it does not necessitate the re-combination of various age-bands into a single chronology unlike the original method (Briffa et al., 2001) and other derived approaches (Scharnweber et al., 2019). The pruned dataset is characterized by an even mean age curve suited for RCS detrending (Esper et al., 2016), and both RCS and SF-RCS were applied to this subset in line with the procedures detailed above for the composite dataset.

2.2. Instrumental data and scaling

Monthly temperatures were extracted at four points centred around 68°N/24°E using the gridded 1.0°x1.0° Berkeley Earth Surface Temperature Anomaly Field (Rohde et al., 2013) accessed through the KNMI climate explorer (<https://climexp.knmi.nl>). The temperature data (Supplementary Fig. S1) were analysed for potential trends using linear regression and by comparing the first (1861–1870) and last decade (1997–2006) of the calibration period. Correlations of the differently detrended composite and living-tree chronologies with monthly average temperature were calculated over a 146-year calibration period from 1861 to 2006.

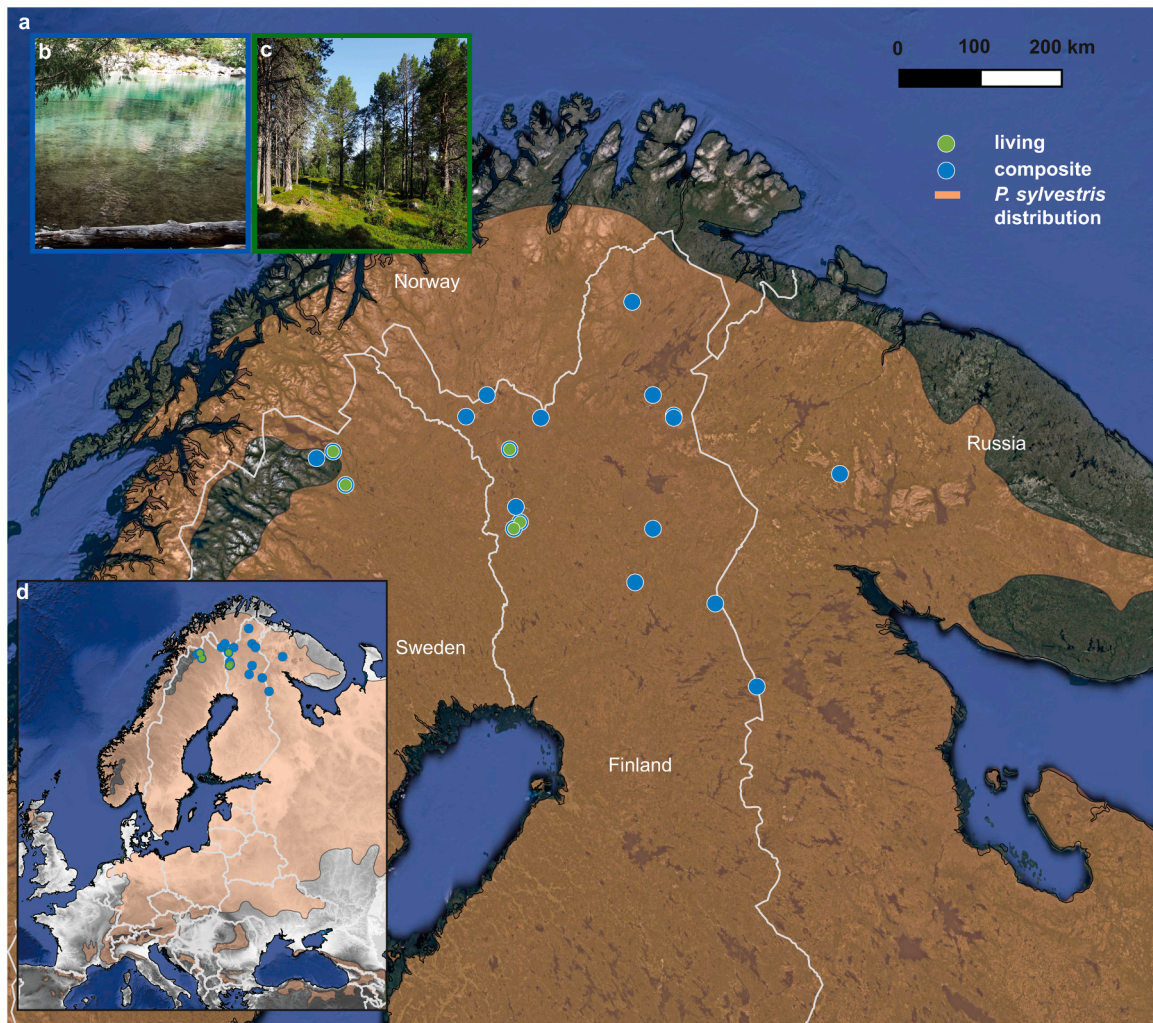


Fig. 1. *Pinus sylvestris* network in northern Scandinavia. a, Fifteen sites used for TRW and MXD composite (blue) and living-tree chronologies (green). Orange area indicates the distribution range of *Pinus sylvestris*. b, Picture of sub-fossil trees from a lake. c, Picture of living trees. d, Overview of the locations in Europe.

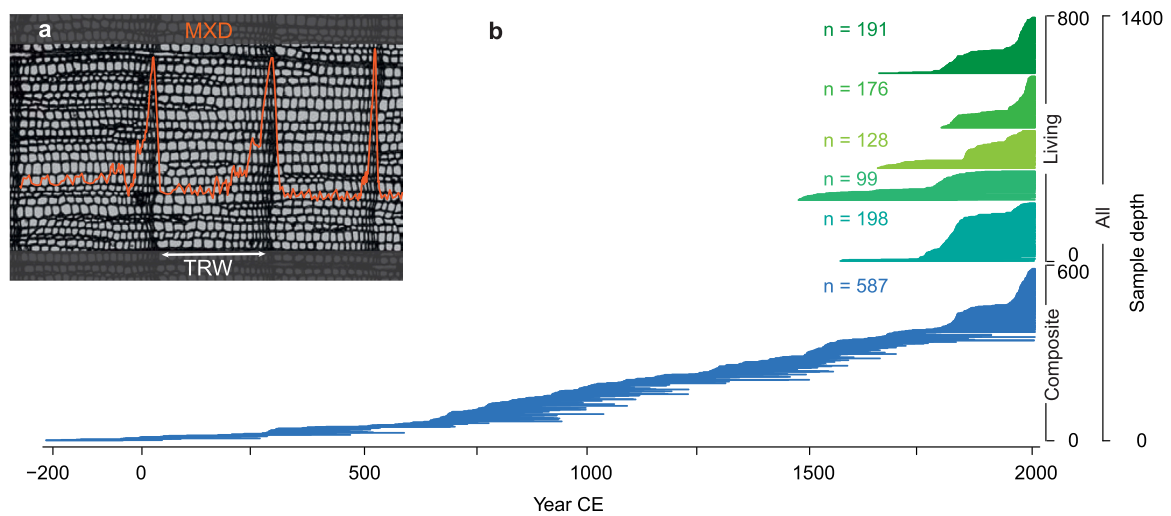


Fig. 2. Changes of replication across sites. a, Thin section showing three tree rings and density profiles (orange curve). b, Sample distribution of the composite dataset in blue and the five living-tree sites in green, with each horizontal line representing one measurement series.

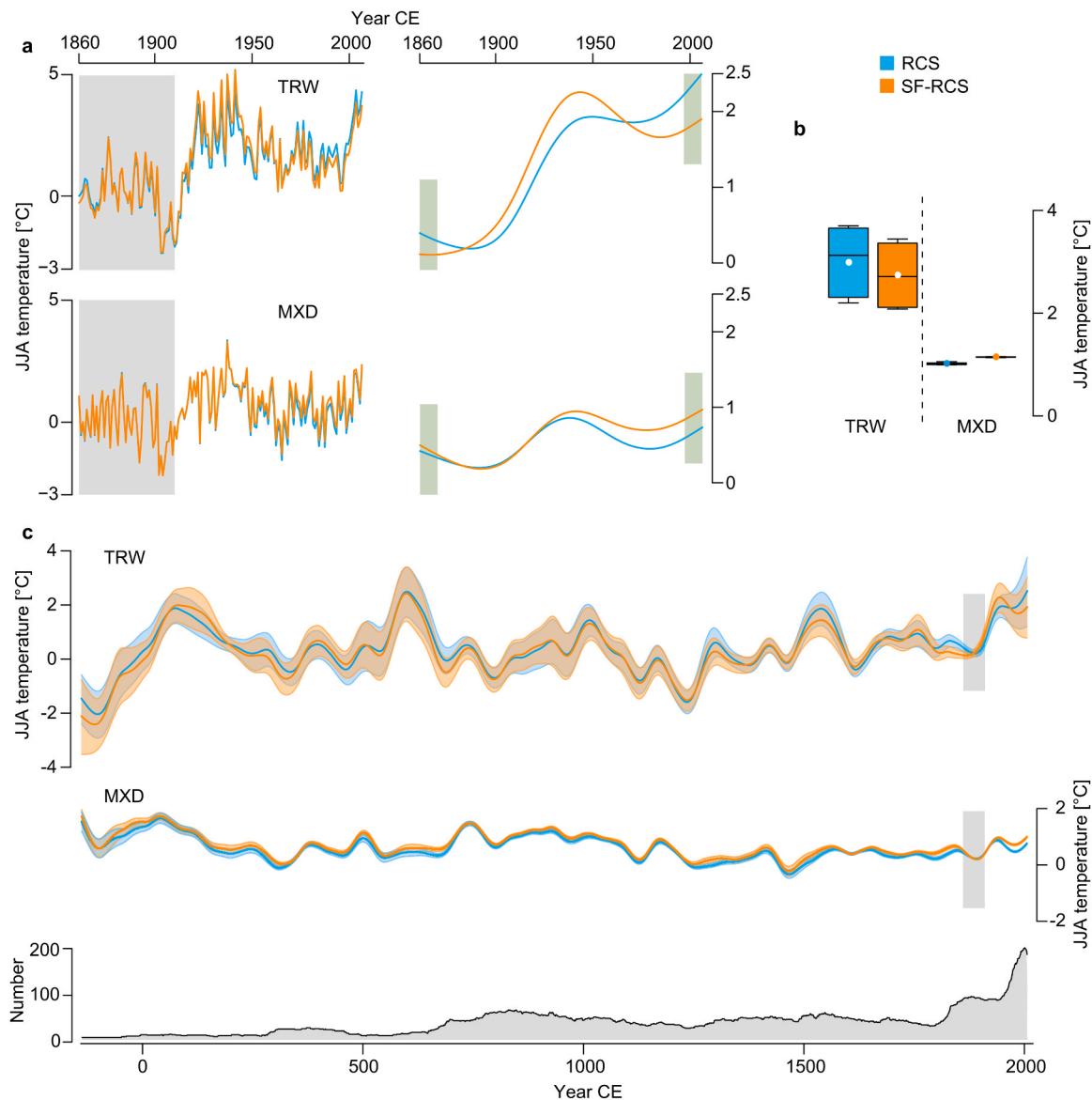


Fig. 3. RCS and SF-RCS detrended composite chronologies from northern Scandinavia. a, TRW (top panel) and MXD chronologies (bottom) after RCS (blue) and SF-RCS detrending (orange) scaled from 1861 to 1910 (grey area) to regional JJA temperature anomalies. Right panels show the same chronologies after smoothing using 100-year spline filters. b, Box plots of the mean temperature changes of scaled TRW and MXD chronologies from 1861 to 1870–1997–2006 (green areas in panel a) considering 12 different RCS (blue) and SF-RCS (orange) detrendings, dots indicate arithmetic means. c, 100-year smoothed RCS (blue) and SF-RCS (orange) TRW and MXD chronologies after scaling the records from 1861 to 1910 (grey areas) to JJA temperature anomalies. Colored bands highlight the variance among the 12 different detrending versions. Bottom panel shows temporal replication changes.

All TRW and MXD chronologies were scaled from 1861 to 1910 to instrumental mean JJA temperatures and expressed as anomalies from the same period. Timeseries were smoothed using 100-year splines to support visual comparison among differently detrended chronologies, TRW and MXD data, composite and living-tree data, and proxy and instrumental data. Temporal changes of reconstructed temperature were again assessed by comparing the means of the first (1861–1870) and last decade (1997–2006) of the calibration period. Residuals between reconstructed and instrumental temperatures were computed to evaluate trends and estimate the skill of differently detrended chronologies.

3. Results

3.1. Basic chronology statistics

Mean segment lengths vary considerably among the various datasets, from 88 to 358 years for the living-tree chronologies, and 136 years for

the composite chronology (not shown). Differences in mean interseries correlations are overall small and centred at $Rbar_{TRW} = 0.59$ and $Rbar_{MXD} = 0.65$ for the composite chronologies, and $Rbar_{TRW} = 0.58$ and $Rbar_{MXD} = 0.68$ for the living-tree chronologies (supplementary Table S2). Both the composite and living-tree mean chronologies show statistically significant correlation ($p < 0.05$) with monthly and seasonal temperatures from June–July, June–August, and July–August over the 1861–2006 calibration period (Büntgen et al., 2011; Esper et al., 2012a, 2012b). The numbers of significant correlations for composite TRW and MXD chronologies are almost identical (19 and 20), but there are differences in magnitude ranging from $r = 0.45$ in TRW up to $r = 0.68$ in MXD (supplementary Fig. S2). Living-tree TRW chronologies show weaker ($r = 0.17–0.29$) and fewer significant correlations (#7) compared to MXD ($r = 0.15–0.60$; #23; supplementary Fig. S3).

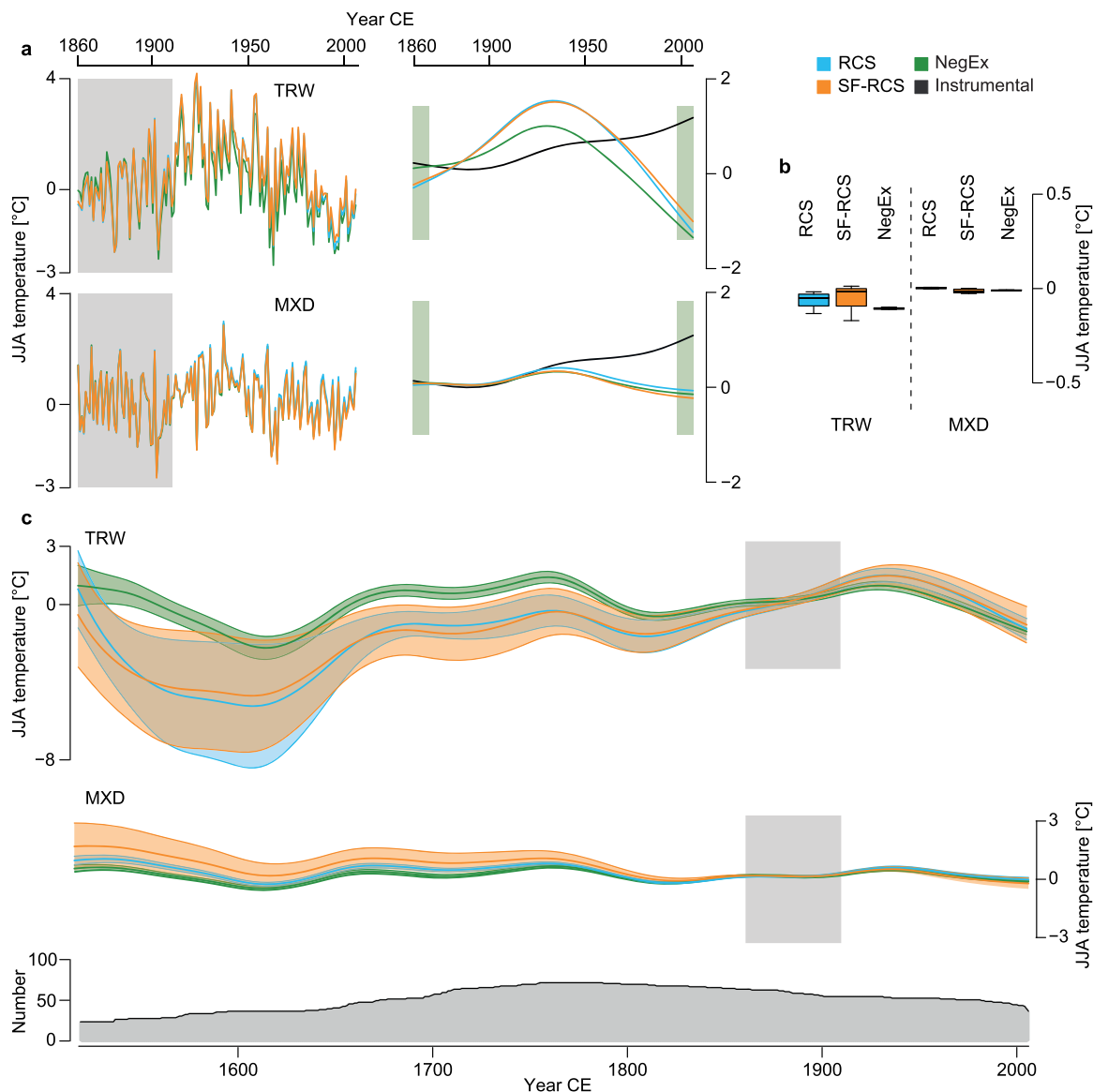


Fig. 4. RCS, SF-RCS and NegEx detrended living-tree chronologies from northern Scandinavia. a, TRW (top panel) and MXD chronologies (bottom) after RCS (blue), SF-RCS (orange) and NegEx detrending (green) scaled from 1861 to 1910 (grey areas) to regional JJA temperature anomalies. Right panels show the same chronologies and instrumental data (black) after smoothing using 100-year spline filters. b, Box plots of mean temperature changes of scaled TRW and MXD chronologies from 1861 to 1870–1997–2006 (green areas in panel a) considering 12 detrendings. c, 100-year smoothed RCS (blue), SF-RCS (orange) and NegEx (green) TRW and MXD chronologies after scaling the records from 1861 to 1910 (grey areas) to JJA temperatures. Colored bands highlight the variance among the 12 different detrending versions. Bottom panel shows temporal replication changes.

3.2. RCS and SF-RCS applied to composite data

RCS and SF-RCS produce larger differences among the 12 chronology versions and between their means when applied to TRW, compared to MXD (Fig. 3). During the 1861–2006 calibration period, the mean TRW RCS and SF-RCS chronologies show only minor differences, yet these are even smaller between the MXD chronologies (Fig. 3a). This conclusion is supported by the residuals between the first and last decade of the calibration period (1861–1870 and 1997–2006) revealing a larger spread among TRW than MXD chronologies, independent of the detrending approach (Fig. 3b). The TRW RCS chronologies show overall greater mean variations than the TRW SF-RCS chronologies, whereas for MXD, this association is reversed, i.e. the SF-RCS chronologies show greater variability than the RCS chronologies. The similarity between RCS and SF-RCS chronology variants remains smaller over the past 2000 in MXD compared to TRW but increases in both proxies during the most recent decades (Fig. 3c).

3.3. Detrending of living-tree datasets and fit with instrumental temperatures

As with the composite dataset, differences caused by detrending living-tree datasets are greater in TRW than in MXD chronologies, although both are larger compared to the composite dataset (Fig. 4). The various chronologies appear largely in agreement during the calibration period (1861–2006), yet major deviations become visible between the TRW NegEx chronology after smoothing the data (right panels in Fig. 4a). However, none of the three mean TRW and MXD chronologies follows the instrumental temperature trend. The comparison of the first and last decade of the calibration period (1861–1870 and 1997–2006) reveals the largest spread in the TRW SF-RCS and RCS chronologies and much smaller differences among the TRW NegEx chronologies (Fig. 4b).

The same analysis shows very little spread among the MXD data. Across the full period from 1521 to 2006, large differences are recorded between the TRW RCS and SF-RCS chronologies compared to the NegEx chronologies (Fig. 4c). Variability among the 12 detrendings increases back in time, a tendency that is more pronounced when applying SF-RCS compared to RCS, while the NegEx shows relatively small differences. Similar to the calibration period, MXD reveals less variability among the 12 detrendings back to 1521. Minor increases back in time are recorded among the SF-RCS detrendings, but the mean timeseries are all in close agreement over the entire period.

3.4. Pruned dataset detrending

The three versions of living-tree datasets show substantial differences in the number of samples and age structure (Fig. 5). The TRW SF-RCS and RCS chronologies of the old dataset show similar patterns that differ increasingly from the NegEx chronology back in time. The three MXD chronologies share similar variability, except the SF-RCS chronology which shows more positive values before 1750. These patterns are also partially retained in the full dataset chronologies (middle panels in Fig. 5), though the differences are overall smaller. Unlike the old dataset, the MXD SF-RCS and RCS chronologies show close agreement throughout the entire period with the NegEx chronology at an almost constant offset. The pruned TRW chronologies largely agree in the mid-section, but differences increase towards both the early and the late chronology periods between NegEx and both RCS and SF-RCS chronologies. The pruned MXD chronologies are more similar, particularly SF-RCS and RCS.

Comparison of the pruned chronologies with the composite chronologies reveals larger differences in TRW compared to MXD (Fig. 6). None of the TRW chronologies match the long-term trend in instrumental temperatures, a feature that also remains in the NegEx detrended

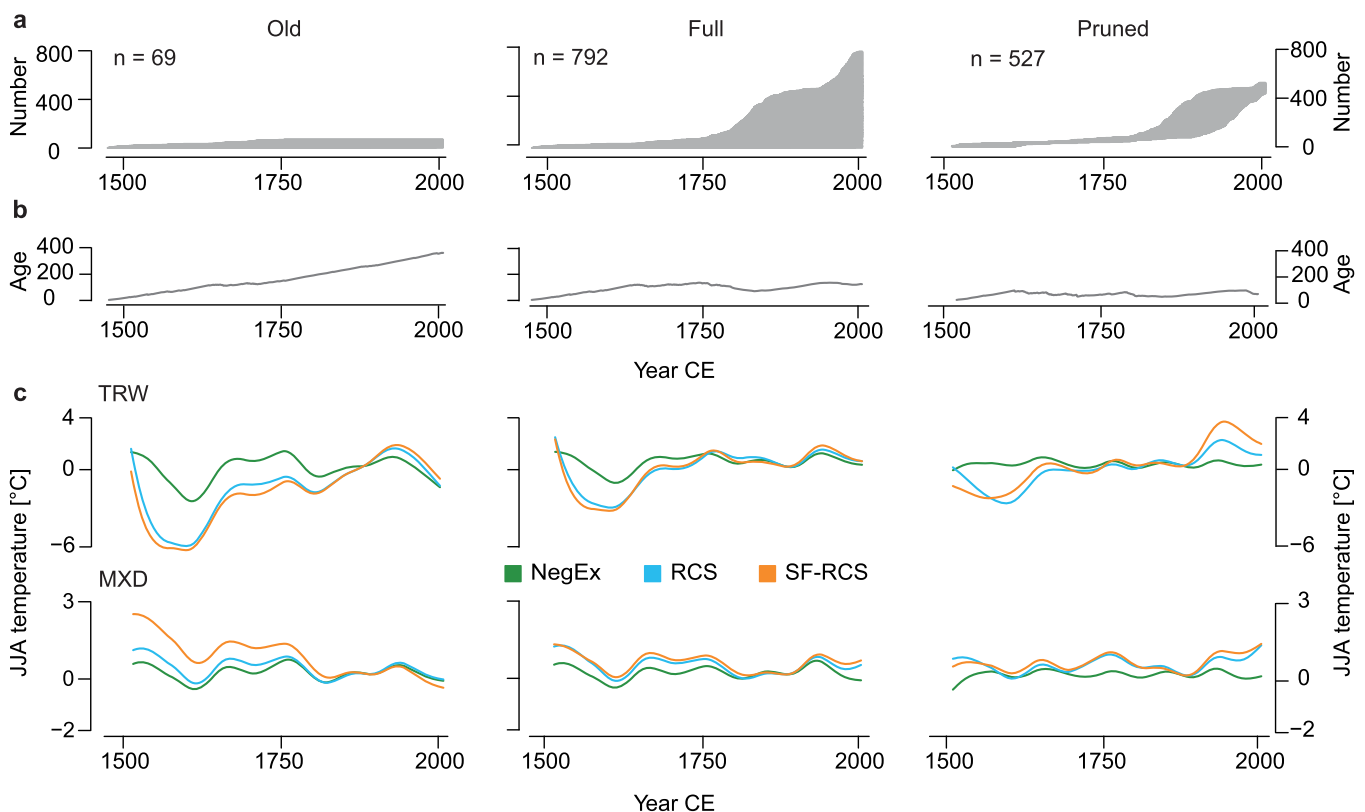


Fig. 5. Influence of replication and age structure on NegEx, RCS and SF-RCS detrended chronologies. a, Temporal changes in replication. b, Mean age curves. c, 100-smoothed TRW- (top) and MXD (bottom) chronologies after NegEx (green), RCS (blue) and SF-RCS detrending (orange) scaled from 1861 to 1910 to regional JJA temperatures.

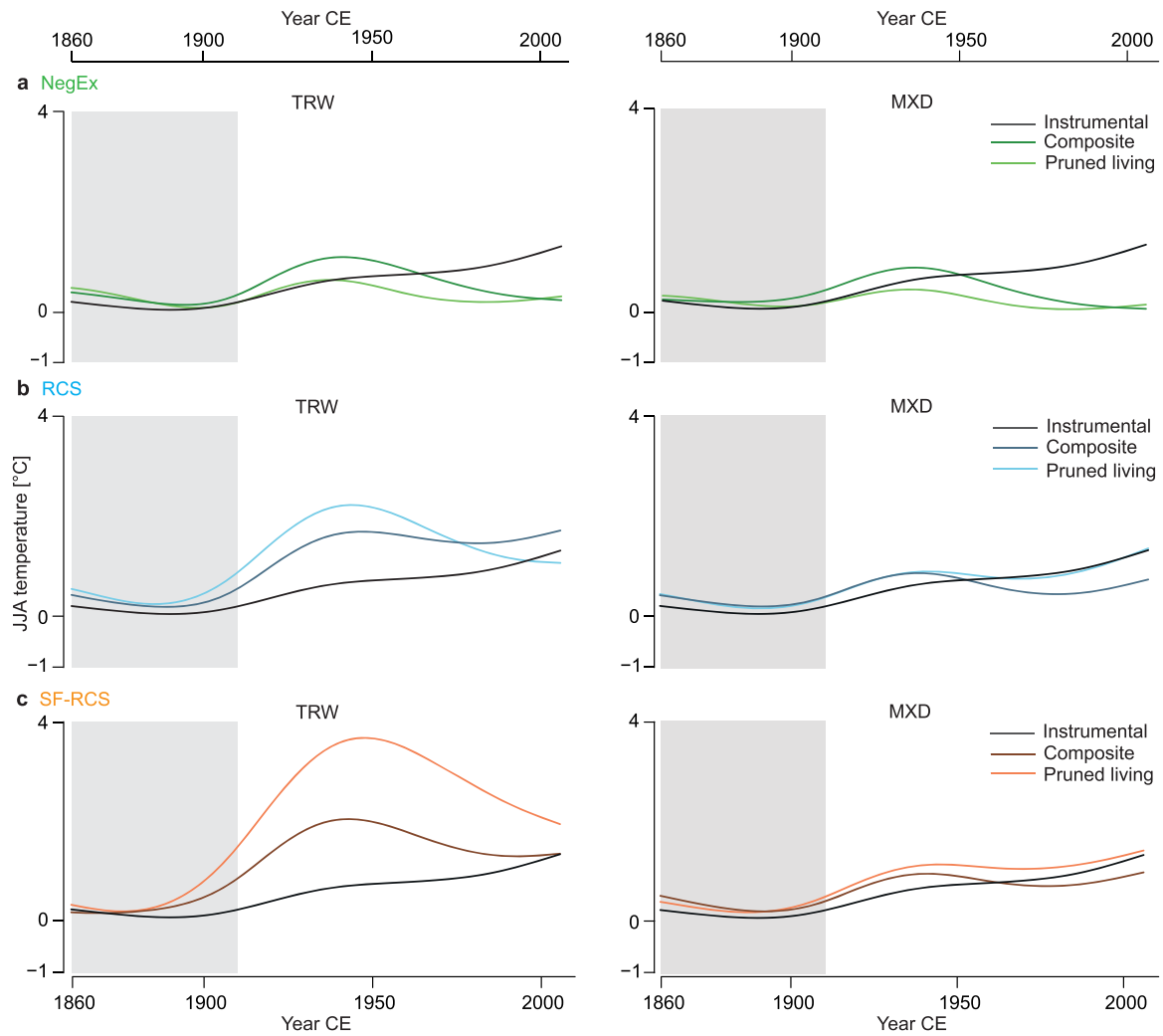


Fig. 6. Influence of age structure on detrending results. a, 100-smoothed TRW (left) and MXD (right) chronologies after NegEx detrending the composite (dark green) and pruned (light green) datasets scaled from 1861 to 1910 (grey areas) to regional JJA temperatures (black). b and c, Same as in a, but for RCS and SF-RCS detrended chronologies, respectively.

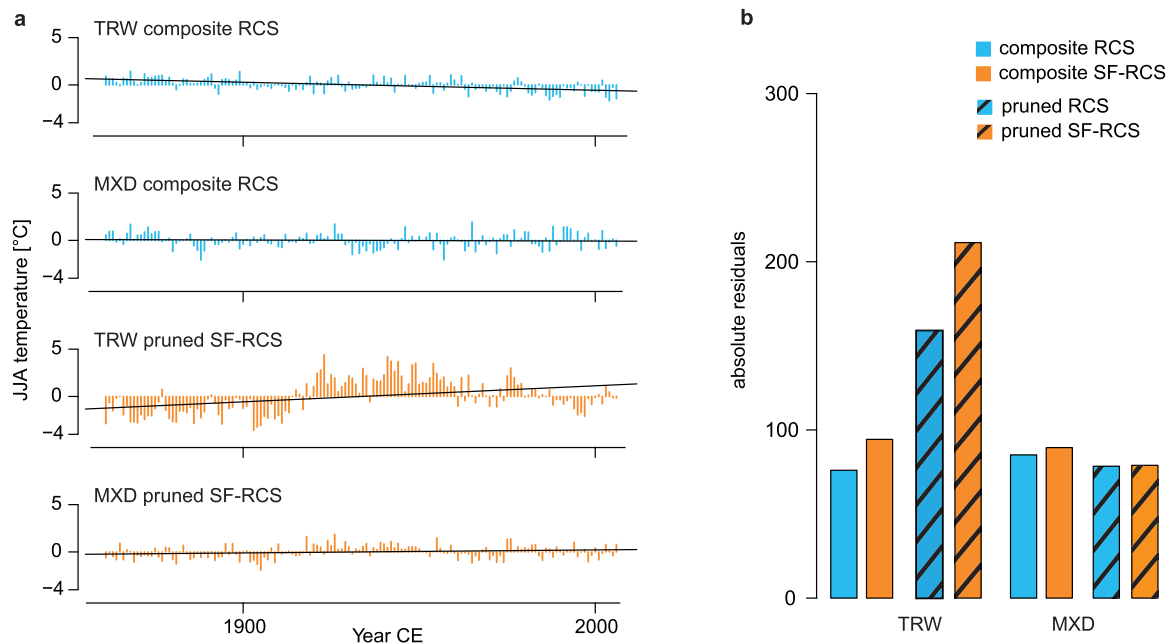


Fig. 7. Residual assessment. **a**, Residuals of differently detrended TRW and MXD chronologies regressed from 1861 to 2006 against instrumental JJA temperatures. **b**, Summed absolute residuals of JJA temperatures and differently detrended TRW and MXD chronologies.

MXD data. Coherent long-term trends are recorded between the instrumental and MXD data after detrending using RCS and SF-RCS. This instrumental-proxy covariance is slightly larger in the pruned living-tree dataset compared to the composite dataset.

3.5. Residual assessment

Considering the best-fit combinations, an assessment of proxy-instrumental residuals reveals minor differences and insignificant trends ($p > 0.05$) for RCS detrended composite MXD and TRW chronologies as well as the pruned SF-RCS detrended living-tree MXD chronology (Fig. 7). The fit is much weaker with the pruned TRW data, and the residual trends are partly opposing between TRW and MXD (supplementary Fig. S4). The various detrendings may cause magnitude differences and are overall more pronounced in SF-RCS. Absolute residuals are substantially larger in pruned TRW data compared to MXD and the composite chronologies (Fig. 7b).

4. Discussion

RCS and SF-RCS have become firmly established as detrending methods with improved preservation of low-frequency climate signals. However, no study compared their influence on TRW and MXD composite and living-tree datasets. Pseudoproxy experiments based on MXD data were used to investigate differences between RCS, SF-RCS, and individual curve detrending concluding that the latter two methods introduced least bias in the final chronologies (Anchukaitis et al., 2013). Other work showed that SF-RCS in combination with age-dependent splines increased coherency between sites of temperature-sensitive chronologies, while moisture-sensitive chronologies did not benefit (McPartland et al., 2020). This study focused on the two most commonly employed applications of RCS excluding numerous variants of the original RCS (overview in Helama et al., 2017). Some of these variants were developed for either TRW or MXD data, while others address additional issues related to low frequency preservation (Björklund et al., 2013; Helama et al., 2017; Nicault et al., 2010). Other more complex RCS variations were not included as limitations associated with original RCS remain standing in case of ensemble standardization (Shi et al., 2020) or a number of method-specific limitations exist as noted for the

DIRECT method (Matskovsky and Helama, 2016). Inclusion of living material of various ages and the large sample depth were used to bypass correction measures for bias introduced by differing or unknown sampling height (Autin et al., 2015). Our comparison of SF-RCS and RCS applied to composite and living TRW and MXD datasets revealed little evidence for a better performance of SF-RCS over RCS, but a generally greater sensitivity of TRW datasets to different detrendings. Application of data pruning is shown to substantially improve chronology covariance and fit with instrumental target data and is particularly recommended as an additional method for living-tree MXD datasets.

Largest detrending differences were found in TRW chronologies during the 20th century, likely linked to the typically higher variance changes inherent to TRW data (Esper et al., 2015) which either remained unadjusted or were treated differently in the 12 detrendings resulting in only minor differences between chronologies (not shown). Despite identical treatment, these differences solely appear in the TRW data where the spread between detrendings is much larger than in MXD (Figs. 3 and 4). Melvin and Briffa (2014) reported less biased chronologies using SF-RCS than RCS for a composite TRW dataset. We, however, produced highly similar chronologies when applying RCS and SF-RCS to composite TRW data. The same is now validated for MXD, for which another study already showed that RCS and SF-RCS created no discernible difference in a temperature reconstruction (Esper et al., 2014). Comparisons using several RCS and correction procedures (Matskovsky, 2011; Matskovsky and Helama, 2014) applied to a composite MXD dataset revealed only minor differences (Matskovsky et al., 2014). However, such an ideal dataset structure composed of living and dead trees is fairly uncommon, as most datasets consist of purely living trees that synchronously age and thereby question the applicability of RCS.

If samples cover a similar timeframe, low-frequency climate related signals might be removed during detrending (Esper et al., 2003; Briffa and Melvin, 2011). However, there are alternative methods to accommodate the use of RCS despite of differing growth rates, multiple origins of sample material, and less than ideal age structures. Grouped or multiple RCS divides the measurement series into subsets to establish separate regional curves which are later re-combined (Esper et al., 2002; Melvin, 2004). However, use of more than two groups entails a loss of absolute amplitudes and some variation of low frequency signal (Briffa

and Melvin, 2011; Helama et al., 2017; Melvin, 2004) and large differences were found for TRW chronologies produced by single RCS and four-curve RCS (Sullivan et al., 2016). Meanwhile pruning truncates the measurement series to emulate the age structure of composite datasets and suit requirements for RCS detrending (Briffa et al., 2001). Our tests using living-tree chronologies reveal larger differences in MXD, particularly with SF-RCS, than previously reported for composite chronologies. A fundamental problem of living-tree datasets is the typically much shorter time period covered by the samples and the lack of young trees, which opposes basic requirements of RCS detrending. Synchronous aging causes a number of problems including the risk of removing meaningful low-frequency climate information regardless of detrending method (Melvin and Briffa, 2014). Our tests show that these limitations account for both TRW and MXD with RCS and SF-RCS applied to living-tree datasets characterized by monotonically increasing mean age curves (see Esper et al., 2016 for an evaluation of mean age curve trends).

This basic limitation can be mitigated by pruning living-tree datasets to emulate the age structure of composite datasets. However, data pruning does not only alter the age structure of a dataset, but also reduces sample replication and frequently the length of a chronology. Even though we combined and used a rather large living-tree dataset for pruning, replication still increased from a low number of samples at the beginning to a higher number of samples towards present, a feature that may generally distort climate signals (Melvin, 2004). The impact of these issues can be seen in the regional curves, where the inclusion of young trees in the full dataset and removal of these in the pruned dataset results in noticeable changes of regional curves (supplementary Fig. S5).

Our results revealed negative effects and reduced covariance with regional temperatures after pruning the living-tree TRW data. However, contrary to the TRW chronologies, both data pruning and SF-RCS detrending produce MXD chronologies with only negligible differences compared to the composite and RCS versions. The pruned RCS and SF-RCS MXD chronologies also capture the trends of regional temperature data, as confirmed in the residual analysis. These marked differences between TRW and MXD demonstrate that the age structure adjustments conducted by pruning living-tree data in concert with RCS and SF-RCS detrending worked only for MXD. While these tests appear overall encouraging and support the prospect of preserving lowest-frequency climate information in living-tree datasets, we need to acknowledge that these results were achieved using a unique collection of homogeneous MXD site chronologies containing a rather strong and coherent temperature signal (Büntgen et al., 2011). Overall, it is essential though that trends in instrumental climate data are accurately captured in tree-ring chronologies. Testing this, e.g., by employing proxy-instrumental residual analyses (Fig. 7) is recommended particularly when changing the age structure of datasets by pruning.

5. Conclusions

Our detrending exercises indicate that great caution is required when detrending living-tree datasets and that these directly influence the interpretation of paleoclimate reconstructions (Büntgen et al., 2021), more so for TRW than for MXD data. Neither simple RCS nor SF-RCS should be applied to such datasets as at best, it risks underestimation of trends in the instrumental data and at worst the detection of opposing trends as demonstrated in a residual analysis. We recommend sampling old and young trees and data pruning as these techniques support preserving potentially meaningful low frequency trends in living-tree datasets. Comparison of RCS and SF-RCS applied to temperature-sensitive tree-ring data revealed minor differences and the applicability of both methods to TRW and MXD composite chronologies, as well as pruned MXD living-tree chronologies. For TRW from solely living trees, neither RCS nor SF-RCS produced robust results and meaningful low-frequency trends coherent with regional temperature data could not be achieved.

CRediT authorship contribution statement

Ulf Büntgen: Writing – review & editing, Conceptualization. **Fredrick Reinig:** Writing – review & editing. **Inga Kirsten Homfeld:** Writing – original draft, Formal analysis, Conceptualization. **Max C.A. Torbenson:** Writing – review & editing. **Jan Esper:** Writing – review & editing, Conceptualization.

Authors statement

I.K.H., U.B., and J.E. conceived and planned the study. I.K.H. conducted the analysis and drafted the manuscript with support by U.B., F.R., M.C.A.T., and J.E. All authors provided discussion and agreed to the final version of the manuscript.

Declaration of Competing Interest

The authors declare that they have no known competing financial interests or personal relationships that could have appeared to influence the work reported in this paper.

Data availability

All data have been uploaded to the International Tree Ring Databank.

Acknowledgments

Supported by the ERC Advanced project MONOSTAR (AdG 882727), the Czech Science Foundation grant HYDRO8 (23–08049 S), and the co-funded EU project AdAgriF (CZ.02.01.01/00/22_008/0004635).

Appendix A. Supporting information

Supplementary data associated with this article can be found in the online version at [doi:10.1016/j.dendro.2024.126205](https://doi.org/10.1016/j.dendro.2024.126205).

References

- Anchukaitis, K.J., D'Arrigo, R.D., Andreu-Hayles, L., Frank, D., Verstege, A., Curtis, A., Buckley, B.M., Jacoby, G.C., Cook, E.R., 2013. Tree-ring-reconstructed summer temperatures from northwestern North America during the last nine centuries. *J. Clim.* 26, 3001–3012. <https://doi.org/10.1175/JCLI-D-11-00139.1>.
- Autin, J., Gennaretti, F., Arseneault, D., Bégin, Y., 2015. Biases in RCS tree ring chronologies due to sampling heights of trees. *Dendrochronologia* 36, 13–22. <https://doi.org/10.1016/j.dendro.2015.08.002>.
- Björklund, J.A., Gunnarson, B.E., Krusic, P.J., Grudd, H., Josefsson, T., Östlund, L., Linderholm, H.W., 2013. Advances towards improved low-frequency tree-ring reconstructions, using an updated *Pinus sylvestris* L. MXD network from the Scandinavian Mountains. *Theor. Appl. Climatol.* 113, 697–710. <https://doi.org/10.1007/s00704-012-0787-7>.
- Briffa, K.R., Jones, P.D., Bartholin, T.S., Eckstein, D., Schweingruber, F.H., Karlén, W., Zetterberg, P., Eronen, M., 1992. Fennoscandian summers from AD 500: temperature changes on short and long timescales. *Clim. Dyn.* 7, 111–119.
- Briffa, K.R., Jones, P.D., Schweingruber, F.H., Karlén, W., Shiyatov, S.G., 1996. Tree-ring variables as proxy-climate indicators: problems with low-frequency signals. In: Jones, P.D., Bradley, R.S., Jouzel, J. (Eds.), *Climatic Variations and Forcing Mechanisms of the Last 2000 Years*. ASI Series. Springer, Berlin, Heidelberg, pp. 9–41. https://doi.org/10.1007/978-3-642-61113-1_2.
- Briffa, K.R., Melvin, T.M., 2011. A Closer Look at Regional Curve Standardization of Tree-ring Records: Justification of the Need, A Warning of Some Pitfalls, and Suggested Improvements in Its Application, in: Hughes, M.K., Diaz, H.F., Swetnam, T.W. (Eds.), *Dendroclimatology: Progress and Prospects, Developments in Paleoenvironmental Research*. Springer Verlag, pp. 113–146.
- Briffa, K.R., Osborn, T.J., Schweingruber, F.H., Harris, I.C., Jones, P.D., Shiyatov, S.G., Vaganov, E.A., 2001. Low-frequency temperature variations from a northern tree ring density network. *J. Geophys. Res.* 106, 2929–2941. <https://doi.org/10.1029/2000JD900617>.
- Bunn, A.G., 2008. A dendrochronology program library in R (dplR). *Dendrochronologia* 26, 115–124. <https://doi.org/10.1016/j.dendro.2008.01.002>.
- Büntgen, U., Allen, K., Anchukaitis, K.J., Arseneault, D., Boucher, É., Bräuning, A., Chatterjee, S., Cherubini, P., Churakova (Sidorova), O.V., Corona, C., Gennaretti, F., Gieseffer, J., Guillet, S., Guiot, J., Gunnarson, B., Helama, S., Hochreuther, P., Hughes, M.K., Huybers, P., Kirilyanov, A.V., Krusic, P.J., Ludescher, J., Meier, W.J.-

- H., Mygland, V.S., Nicolussi, K., Oppenheimer, C., Reinig, F., Salzer, M.W., Seftigen, K., Stine, A.R., Stoffel, M., St. George, S., Tejedor, E., Trevino, A., Trouet, V., Wang, J., Wilson, R., Yang, B., Xu, G., Esper, J., 2021. The influence of decision-making in tree ring-based climate reconstructions. *Nat. Commun.* 12, 3411. <https://doi.org/10.1038/s41467-021-23627-6>.
- Büntgen, U., Raible, C.C., Frank, D.C., Helama, S., Cunningham, L., Hofer, D., Nievergelt, D., Verstege, A., Timonen, M., Stenseth, N.C., Esper, J., 2011. Causes and consequences of past and projected Scandinavian summer temperatures, 500–2100 AD. *PLOS ONE* 6, e25133. <https://doi.org/10.1371/journal.pone.0025133>.
- Cook, E.R., 1985. A Time Series Approach to Tree-ring Standardization (PhD Thesis). University of Arizona, Tucson, AZ, USA.
- Cook, E.R., 1987. The decomposition of tree-ring series for environmental studies. *Tree-Ring Bull.* 47, 37–59.
- Cook, E.R., Briffa, K.R., Meko, D.M., Graybill, D.A., Funkhouser, G., 1995. The segment length curve in long tree-ring chronology development for paleoclimatic studies. *Holocene* 5, 229–237.
- Cook, E.R., Kairiukstis, L.A., 1990. *Methods of Dendrochronology: Applications in the Environmental Sciences*. Springer Science & Business Media.
- Cook, E.R., Krusic, P.J., Peters, K., Holmes, R.L., 2017a. Program ARSTAN (version 41), Autoregressive tree-ring standardization program.
- Cook, E.R., Krusic, P.J., Peters, K., Melvin, T., 2017b. Program Signal Free (version 45_v2b), RCS Signal Free tree-ring standardization program.
- Cook, E.R., Peters, K., 1981. The smoothing spline: a new approach to standardizing forest interior tree-ring width series for dendroclimatic studies. *Tree-Ring Bull.* 41, 45–53.
- Cook, E.R., Peters, K., 1997. Calculating unbiased tree-ring indices for the study of climatic and environmental change. *Holocene* 7, 361–370.
- Cooper, M.G., Nolin, A.W., Safeeq, M., 2016. Testing the recent snow drought as an analog for climate warming sensitivity of Cascades snowpacks. *Environ. Res. Lett.* 11, 084009. <https://doi.org/10.1088/1748-9326/11/8/084009>.
- Core Team, R., 2022. R: A Language and Environment for Statistical Computing.
- Esper, J., Büntgen, U., Timonen, M., Frank, D.C., 2012a. Variability and extremes of northern Scandinavian summer temperatures over the past two millennia. *Glob. Planet. Change* 88–89, 1–9. <https://doi.org/10.1016/j.gloplacha.2012.01.006>.
- Esper, J., Cook, E.R., Schweingruber, F.H., 2002. Low-frequency signals in long tree-ring chronologies for reconstructing past temperature variability. *Science* 295, 2250–2253. <https://doi.org/10.1126/science.1066208>.
- Esper, J., Cook, E.R., Krusic, P.J., Peters, K., Schweingruber, F.H., 2003. Tests of the RCS method for preserving low-frequency variability in long tree-ring chronologies. *Tree-Ring Res.* 59, 81–98.
- Esper, J., Dühorn, E., Krusic, P.J., Timonen, M., Büntgen, U., 2014. Northern European summer temperature variations over the Common Era from integrated tree-ring density records. *J. Quat. Sci.* 29, 487–494. <https://doi.org/10.1002/jqs.2726>.
- Esper, J., Frank, D.C., Timonen, M., Zorita, E., Wilson, R.J.S., Luterbacher, J., Holzhammer, S., Fischer, N., Wagner, S., Nievergelt, D., Verstege, A., Büntgen, U., 2012b. Orbital forcing of tree-ring data. *Nat. Clim. Change* 2, 862–866. <https://doi.org/10.1038/nclimate1589>.
- Esper, J., Krusic, P.J., Ljungqvist, F.C., Luterbacher, J., Carrer, M., Cook, E.R., Davi, N.K., Hartl-Meier, C., Kiryanov, A., Konter, O., Mygland, V., Timonen, M., Treyde, K., Trouet, V., Villalba, R., Yang, B., Büntgen, U., 2016. Ranking of tree-ring based temperature reconstructions of the past millennium. *Quat. Sci. Rev.* 145, 134–151. <https://doi.org/10.1016/j.quascirev.2016.05.009>.
- Esper, J., Schneider, L., Smerdon, J.E., Schöne, B.R., Büntgen, U., 2015. Signals and memory in tree-ring width and density data. *Dendrochronologia* 35, 62–70. <https://doi.org/10.1016/j.dendro.2015.07.001>.
- Frank, D.C., Esper, J., Cook, E.R., 2007. Adjustment for proxy number and coherence in a large-scale temperature reconstruction. *Geophys. Res. Lett.* 34. <https://doi.org/10.1029/2007GL030571>.
- Fritts, H.C., 1976. *Tree Rings and Climate*. Academic Press, New York.
- Fritts, H.C., Mosimann, J.E., Bottorff, C.P., 1969. A Revised Computer Program for Standardizing Tree-Ring Series. *Tree-Ring Bull.*
- Gunnarson, B.E., Linderholm, H.W., Moberg, A., 2011. Improving a tree-ring reconstruction from west-central Scandinavia: 900 years of warm-season temperatures. *Clim. Dyn.* 36, 97–108. <https://doi.org/10.1007/s00382-010-0783-5>.
- Helama, S., Melvin, T.M., Briffa, K.R., 2017. Regional curve standardization: state of the art. *Holocene* 27, 172–177. <https://doi.org/10.1177/0959683616652709>.
- Holmes, R.L., 1983. Computer assisted quality control in tree-ring dating and measurement. *Tree-Ring Bull.* 43, 69–78.
- Linderholm, H.W., Björklund, J.A., Seftigen, K., Gunnarson, B.E., Grudd, H., Jeong, J.-H., Drobyshev, I., Liu, Y., 2010. Dendroclimatology in Fennoscandia – from past accomplishments to future potential. *Climate* 6, 93–114. <https://doi.org/10.5194/cp-6-93-2010>.
- Matskovsky, V., 2011. Estimation of biases in RCS chronologies of tree rings. *J. Sib. Fed. Univ. Biol.* 389–404.
- Matskovsky, V., Helama, S., 2014. Testing long-term summer temperature reconstruction based on maximum density chronologies obtained by reanalysis of tree-ring data sets from northernmost Sweden and Finland. *Climate* 10, 1473–1487. <https://doi.org/10.5194/cp-10-1473-2014>.
- Matskovsky, V., Helama, S., 2016. Direct transformation of tree-ring measurements into palaeoclimate reconstructions in three-dimensional space. *Holocene* 26, 439–449. <https://doi.org/10.1177/0959683615609748>.
- McPartland, M.Y., St. George, S., Pederson, G.T., Anchukaitis, K.J., 2020. Does signal-free detrending increase chronology coherence in large tree-ring networks? *Dendrochronologia* 63, 125755. <https://doi.org/10.1016/j.dendro.2020.125755>.
- Melvin, T.M., 2004. Historical Growth Rates and Changing Climatic Sensitivity of Boreal Conifers (PhD Thesis). University of East Anglia, Norwich, United Kingdom.
- Melvin, T.M., Briffa, K.R., 2008. A 'signal-free' approach to dendroclimatic standardisation. *Dendrochronologia* 26, 71–86.
- Melvin, T.M., Briffa, K.R., 2014. CRUST: software for the implementation of regional chronology standardisation: Part 1. signal-free RCS. *Dendrochronologia* 32, 7–20. <https://doi.org/10.1016/j.dendro.2013.06.002>.
- Melvin, T.M., Grudd, H., Briffa, K.R., 2013. Potential bias in 'updating' tree-ring chronologies using regional curve standardisation: re-processing 1500 years of Torneträsk density and ring-width data. *Holocene* 23, 364–373. <https://doi.org/10.1177/0959683612460791>.
- Nehrbass-Ahles, C., Babst, F., Klesse, S., Nötzli, M., Bouriaud, O., Neukom, R., Dobbertin, M., Frank, D.C., 2014. The influence of sampling design on tree-ring-based quantification of forest growth. *Glob. Change Biol.* 20, 2867–2885. <https://doi.org/10.1111/gcb.12599>.
- Nicault, A., Guiot, J., Edouard, J.L., Brewer, S., 2010. Preserving long-term fluctuations in standardisation of tree-ring series by the adaptive regional growth curve (ARGC). *Dendrochronologia* 28, 1–12. <https://doi.org/10.1016/j.dendro.2008.02.003>.
- Rohde, R., A. Muller, R., Jacobsen, R., Muller, E., Wickham, C., 2013. A new estimate of the average Earth surface land temperature spanning 1753 to 2011. *Geoinf. Geostat. Overv.* 01. <https://doi.org/10.4172/2327-4581.1000101>.
- Römer, P., Hartl, C., Schneider, L., Bräuning, A., Szymczak, S., Huneau, F., Lebre, S., Reinig, F., Büntgen, U., Esper, J., 2021. Reduced temperature sensitivity of maximum latewood density formation in high-elevation Corsican pines under recent warming. *Atmosphere* 12. <https://doi.org/10.3390/atmos12070804>.
- Scharnweber, T., Heußner, K.-U., Smiljanic, M., Heinrich, I., van der Maaten-Theuissen, M., van der Maaten, E., Struwe, T., Buras, A., Wilmking, M., 2019. Removing the no-analogue bias in modern accelerated tree growth leads to stronger medieval drought. *Sci. Rep.* 9, 2509. <https://doi.org/10.1038/s41598-019-39040-5>.
- Shi, F., Yang, B., Linderholm, H.W., Seftigen, K., Yang, F., Yin, Q., Shao, X., Guo, Z., 2020. Ensemble standardization constraints on the influence of the tree growth trends in dendroclimatology. *Clim. Dyn.* 54, 3387–3404. <https://doi.org/10.1007/s00382-020-05179-5>.
- St. George, S., 2014. An overview of tree-ring width records across the Northern Hemisphere. *Quat. Sci. Rev.* 95, 132–150. <https://doi.org/10.1016/j.quascirev.2014.04.029>.
- Sullivan, P.F., Pattison, R.R., Brownlee, A.H., Cahoon, S.M.P., Hollingsworth, T.N., 2016. Effect of tree-ring detrending method on apparent growth trends of black and white spruce in interior Alaska. *Environ. Res. Lett.* 11, 114007. <https://doi.org/10.1088/1748-9326/11/11/114007>.
- Wang, J., Yang, B., Qin, C., Kang, S., He, M., Wang, Z., 2014. Tree-ring inferred annual mean temperature variations on the southeastern Tibetan Plateau during the last millennium and their relationships with the Atlantic Multidecadal Oscillation. *Clim. Dyn.* 43, 627–640. <https://doi.org/10.1007/s00382-013-1802-0>.
- Wilson, R.J.S., Anchukaitis, K.J., Briffa, K.R., Büntgen, U., Cook, E.R., D'Arrigo, R., Davi, N., Esper, J., Frank, D.C., Gunnarson, B., Hegerl, G., Helama, S., Klesse, S., Krusic, P.J., Linderholm, H.W., Mygland, V., Osborn, T.J., Rydval, M., Schneider, L., Schurer, A., Wiles, G., Zhang, P., Zorita, E., 2016. Last millennium northern hemisphere summer temperatures from tree rings: Part I: the long term context. *Quat. Sci. Rev.* 134, 1–18. <https://doi.org/10.1016/j.quascirev.2015.12.005>.
- Wilson, R.J.S., Miles, D., Loader, N.J., Melvin, T., Cunningham, L., Cooper, R., Briffa, K.R., 2012. A millennial long March–July precipitation reconstruction for southern-central England. *Clim. Dyn.* 1–21.
- Zang, C., Biondi, F., 2015. treeclim: an R package for the numerical calibration of proxy-climate relationships. *Ecography* 38, 431–436. <https://doi.org/10.1111/ecog.01335>.
- Zhang, H., Shao, X., Zhang, Y., 2015. Which climatic factors limit radial growth of Qilian juniper at the upper treeline on the northeastern Tibetan Plateau? *J. Geogr. Sci.* 25, 1173–1182. <https://doi.org/10.1007/s11442-015-1226-3>.
- Zhao, S., Pederson, N., D'Orangeville, L., HilleRisLambers, J., Boose, E., Penone, C., Bauer, B., Jiang, Y., Manzanedo, R.D., 2019. The international Tree-Ring data bank (ITRDB) revisited: data availability and global ecological representativity. *J. Biogeogr.* 46, 355–368. <https://doi.org/10.1111/jbi.13488>.